Int J Adv Manuf Technol (2002) 19:850–858
Ownership and Copyright

The International Journal of Advanced Manufacturing Technology

A Study of High-Precision CNC Lathe Thermal Errors and Compensation

P.-C. Tseng and J.-L. Ho

Department of Mechanical Engineering, National Chung-Hsing University, Taichung, Taiwan

This study is addressed at the thermal deformation errors resulting from temperature rise that contribute to 40%–70% of the precision errors in machining at a turning centre, and proposes an economic, accurate, and quick measurement method. It also investigates the thermal error differentials between static idle turning and in the actual cutting environment. The temperature measurement units are intelligent IC temperature sensors with correction circuits. The A/D card extracts and transforms data and saves data in the computer files, and the displacement sensor measures the displacement deviation online during cutting. The temperatures and the deviation of thermal drifts so obtained are used to establish the relationship function using multivariable linear regression and nonlinear exponential regression models, respectively. Finally, this paper compares software compensation methods for the thermal-drift relationship. As proven by experiments, the software compensation method can limit the thermal error of a turning centre to within 5 μm. Moreover, the software compensation for the thermal error relationship using a single variable nonlinear exponent regression model can reduce the error by 40% to 60%.

Keywords: Compensation method; Deformation; Regression model; Sensor; Thermal errors

1. Introduction

Using systematic methods to reduce the CNC machine tool errors, improve product precision and thus increase the value added to the products has become an important area of study. This study targets the thermal deformation errors resulting from temperature rise that contribute 40%–70% of the precision error in machining in a turning centre. Further, the study proposes an economic, accurate, and quick measuring method for obtaining the temperature rise and thermal drift values, in order to establish the relationship between geometric error and temperature for a turning centre. The use of the software compensation method to improve the precision of machined products is the subject of this paper.

According to Bryan [1,2], the thermal errors of a machine tool arise from six sources, i.e. heat produced in the cutting process, energy lost in the mechanical system, the cooling system, change of room temperature, operation of the machine tool, and thermal memory effect. Although much research on thermal errors has been carried out since 1967, little improvement in the thermal errors of machine tools was achieved until 1990. The solutions to the thermal errors of machine tools are concentrated on the following three aspects: reduction in the heat sources, control over the direction of heat transmission, and design of a thermally robust structure. Some manufacturers have produced machine tools with air bearings. Since the component parts inside the bearing do not have direct contact with each other, the configuration provides a solution to the problem of generating heat from friction in the traditional roller bearing. Although there has been work on thermal errors of machine tools since 1960, most of the literature is devoted to CNC machining centres [3–7] and few papers mentioned the turning centres [8–10]. This is because thermal error measuring methods and techniques applied to machining centres cannot be used for turning centres. The reasons can be summarised as follows:

1. The difficulty of measuring equipment set-up. With the normal machining dimensions, it is not easy to set up the equipment for the error measurement in a turning centre owing to the limited space. Therefore, error measurement is more difficult for a turning centre than for a machining centre. In addition, the lathe turret tends to produce interference and cause collisions.
2. Symmetric structure. The H-type turning centre is a symmetric structure, so its thermal error effect is not as obvious as that from a V-type machining centre, which in turn causes extra difficulties in building an accurate model of thermal drift. According to reports by machine tool manufacturers, the axial errors of a lathe within 100–200 μm should be corrected on the basis of the relationship between temperature and displacement.
3. Measurement benchmark. It is hard to find a measurement benchmark for a turning centre, which is different from the

Correspondence and offprint requests to: Dr. P.-C. Tseng, CIM Laboratory, National Chung-Hsing University, 250 Kuo-Kung Road, Tai-Chung City, Taiwan 40227. E-mail: pctseng@dragon.nchu.edu.tw

machining centre. Hence, laser interferometer equipment has to be used. However, it is still not easy to make the correction by laser interferometer equipment because of unparalleled-axes scale errors.

In the literature related to compensation methods for turning centres, only the analogue method developed by Domez [11] is close to completion. It adds analogue compensation signals to the driving signals of the servo motor in order to realise the compensation. However, this work targets compensation using an open-loop controller and is thus not appropriate to the currently more popular, but more restricting FANUC controller. The reason is that the FANUC controller uses digital servo signals without the involvement of other external signals in the feedback loop. Therefore, finding a quick measurement and compensation method are desired technologies.

This study will be based on quick measurement of the relative values of temperature increase and thermal deformation, establish the relationship between geometric errors and the temperatures of a turning centre, and then use a software compensation method to improve product machining precision and add value to the turning centre.

The functions of the system are described in brief below:

1. Use the IC-AD590 temperature sensor to measure the temperature, and the A/D card to extract data and transform signals.
2. Use the LTO2S circular displacement apparatus on the lathe to measure the displacement.
3. Establish the thermal error model based on actual cutting.
4. Establish the thermal error model using linear and nonlinear regression analysis.
5. Compare and develop simple thermal-error compensation methods for a turning centre.

2. Deformation Impact on Machining Precision and the Countermove

In order to simplify the thermal error model for a turning centre, early work shows that the focus may be placed on such critical component parts as the spindle and the servo axis of tool carriage that have direct impact on the precision of the machining parts [12,13].

2.1 Spindle Thermal Drift at the Turning Centre

An H-type spindle bearing, has a radial bearing both at the front and at the rear of the spindle to resist the cutting force. In order to avoid the thrust from radial turning, the back of the spindle is equipped with a thrust bearing. Thus, there is only one set of thrust bearings that can prevent the spindle displacement resulting from the increase in temperature in the radial direction on both end bearings. This design places a limit on the rear part of the spindle while leaving room for the front part to extend, thus causing the following three cases of spindle thermal deformation due to temperature rise:

1. Only axial forward extension occurs. The reason for this type of deformation is the axial temperature rise of the spindle housing or the spindle, and the *Z*-axial displacement of both against the machine datum.
2. The spindle has simultaneous axial and radial thermal displacement. The radial thermal displacement could be upward (*Y*-axis) or horizontal (*X*-axis), the reason for which is that the spindle box has a thermal displacement in two directions simultaneously and is combined with the spindle's *Z*-axis thermal displacement.
3. The divergence of spindle axis centre is caused by thermal deformation due to the unequal bearing temperature rise at the front and back bearings. This can be so serious that it makes high-speed running very dangerous. This error is hard to compensate for.

2.2 Thermal Drift of Servo Axis at the Turning Centre

The turret is inserted on a ball screw, and the positioning precision, straightness, and perpendicularity have become the major determinants of the actual location of the cutting tip, together with the stick slip friction, the static and dynamic rigidity of the guideways, and the servo motor's sensitivity to small incremental feeds. The ball screw's temperature will increase with frequent fast moves, or heavy-loaded cutting, or heat transmission from external sources, and the bearings on the two fixed ends will cause deformation and then bending of the ball screw. Therefore, the cutter turret has not only parallel movement in two directions, but also produces Ábbe offset errors. Fortunately, it will only cause a parallel movement of the cutter end in two directions to the rotational axis of a single-point cutter, which can be compensated for using HTM computation. The errors will not cause a deviation of the working point. However, the errors caused by ball screw deformation and bending will cause a dynamic cutting tool in C-axial machining to overcut the component part or produce errors when shaping component parts.

The servo axes of the turning centre are comprised of two servo motors each with ball screws. One is the *X*-axis and the other is the *Z*-axis. The error is the combination of the two. The thermal error is more complicated than that for a single shaft. Therefore, the selection of appropriate bearings and spindle shaft provides the optimal solution to improving ball screw errors. With regard to the thermal errors of the turning centre caused by the components with high friction, high-speed rotation or movement (e.g. transmission axis, linear slide, high-speed spindle), there are three ways to improve this:

1. Prevent heat transmission.
2. Reduce or prevent thermal deformation.
3. Compensate after thermal deformation.

The approach of individual machine tool manufacturers depends on individual technical level.

2.3 Other Errors of the Turning Centres

1. Quasi-static errors. Slowly changing and increasing errors after using machines after delivery, including geometric errors, kinematics errors, the errors caused by external

attachments, inappropriate mechanic assembly, unstable materials, and improper sensor apparatus.

2. Dynamic forces errors. The vibration of the mechanical structure attributable to sources of dynamic forces cause errors on the surface of the component part.
3. Impact of cutting tool deformation on precision machining. The proportion of the heat transmitted to the machine tool is small compared to the total amount of heat generated during cutting. However, it still causes the temperature to rise owing to the small volume and thermal capacity of the cutting tool. When the cutting tool temperature rises the heating causes a volume expansion and eventually causes machining errors.

For static error improvement of a machine tool, HTM can be used to represent the errors caused by an imperfect rotating axis in a turning centre lathe [14]. A perpendicular Z-axis radial movement exists with respect to the rotating axis. The deflection from inaccurate clamping of components, axial movement parallel to the Z-axis, and oscillation with an error in terms of the angle from the Z-axis all cause inaccuracy in the relative position of the moving parts. A description of the errors and moving parts of these moving objects may be realised by converting and computing the object's movement features relative to a datum coordinate. Such a conversion relationship can be represented by 4×4 HTM. The product of HTM refers to continuous coordinate conversion.

$$^{0}T_N = \prod_{m=1}^{N} T_m = T_1T_2T_3\ldots T_N \qquad (1)$$

There are six errors in the degrees of freedom of the spindle of a turning centre. θ_z is the revolution angle of the Z-axis; δ_x is the error of parallel movement of the X-axis; δ_y is the error of parallel movement of the Y-axis; δ_z is the error of parallel movement of the Z axis; ϵ_x is the revolution error of the X-axis; and ϵ_y is the revolution error of the Y-axis. T_1 represents a parallel movement to the X-axis by x; T_2 represents a parallel movement to the Y-axis by y; T_3 represents a parallel movement to the Z-axis by z; T_4 represents a revolution of the X-axis by q_x; T_5 represents a revolution of the Y-axis by q_y; and T_6 represents a revolution of the Z-axis by q_z. Hence, the HTM of the spindle's errors can be written as:

$$^{0}T_N = \prod_{m=1}^{N} T_m = T_1T_2T_3T_4T_5T_6 \qquad (2)$$

For the high-speed spindle of a turning centre, θ_z is a function of time, denoted by $\theta_z(t)$, due to the high-speed of the revolution feature. Because $\theta_z(t)$ changes very fast, the resulting errors cannot be compensated for immediately. The errors of the spindle of a turning centre can thus be simplified as:

$$^{0}T_N = \prod_{m=1}^{N} T_m = T_1T_2T_3T_4T_5 \qquad (3)$$

The error HTM for the spindle of the turning centre after the computation with inputs of the revolution and parallel movement matrices can be represented by:

$$\begin{bmatrix} X \\ Y \\ Z \\ 1 \end{bmatrix}_{error} = {}^{XYZ}T_{X_1Y_1Z1} \begin{bmatrix} X \\ Y \\ Z \\ 1 \end{bmatrix} \qquad (4)$$

The turning centre has two servo axes, the X-axis and the Z-axis, while the X-axis is mounted on the Z-axis. Based on the HTM after coordinate conversion, the following error converting matrix of the cutting tool's actual and ideal positions can be obtained:

$$\begin{bmatrix} \delta_{x_t} \\ \delta_{y_t} \\ \delta_{z_t} \end{bmatrix}_{actual} = \begin{bmatrix} X_t \\ Y_t \\ Z_t \end{bmatrix}_{actual} - \begin{bmatrix} X_t \\ Y_t \\ Z_t \end{bmatrix}_{ideal} \qquad (5)$$

For the turning centre, the actual machining error is the total of the cutting tool's error and the component part's error:

$$\begin{bmatrix} X_\delta \\ Y_\delta \\ Z_\delta \\ 1 \end{bmatrix}_{REAL} = \begin{bmatrix} \delta_{x_t} \\ \delta_{y_t} \\ \delta_{z_t} \\ 1 \end{bmatrix}_{actual} + \begin{bmatrix} X \\ Y \\ Z \\ 1 \end{bmatrix}_{error} \qquad (6)$$

Micro adjustment when assembling the machine tool can correct the static errors and reduce the modelling and measuring time, and make on-line improvement by tracing the system's errors over time. However, the thermal deformation errors of a machine tool, as reflected in Eq. (5), cannot be corrected by static compensation. The complicated relationship between temperature and deformation must be derived from experiments, and improved by on-line real-time measurement.

3. Experiment Equipment and the Measurement System

3.1 Temperature Measurement

There are many types of temperature sensor [10]. This experiment uses on IC sensor AD 590 with an output of 1 μ A °C^{-1} to measure the temperature. It has good linearity, wide power range (+4 V–+30 V), and is small and easy to install so that no compensating circuit is needed. It is able to test a temperature range of about −55°C–150°C. The locations for temperature measuring in this experiment include spindle, ball screw, turret, cutting space, and room temperature. For the spindle as a whole, all the bearings are sources of heat. The ball screw affects the positioning precision and the turret has an impact on the cutting tool's temperature when cutting. Consequently, all these items should be measured. The distribution of the eight locations is shown in Table 1.

3.2 Displacement Measuring System

To implement a simple, easy, fast and accurate method to obtain highly reliable data, a RENISHAW-LTO2S lathe using

Table 1. The number and location of the parts for temperature measurement.

Number	Location	Number	Location
Ch1(T_1)	2nd Bearing on spindle	Ch5(T_5)	End of spindle
Ch2(T_2)	3rd Bearing on spindle	Ch6(T_6)	1st Bearing on spindle
Ch3(T_3)	Ball screw	Ch7(T_7)	Turret
Ch4(T_4)	Cutting space	Ch8(T_8)	Room temperature

a circular displacement measurement was hired. This apparatus consists of an OMM (optical module machine), an OMP (optical module probe) and an MI12 interface. The measuring probe relies on a clamp to fix it on to the turret. When the MI12 is activated, the OMP sends and the OMM receives infrared signals so as to reach a balanced state. When the probe touches the component part, the internal resistor connected to the base of the probe changes and cuts off the infrared signals from the probe. This output end is connected to the skip signal of the machine tool so that the machine tool will be informed through the PMC (programmable machine controller) to stop execution of the current NC code. By MACRO, the machine tool will also be able to read the mechanic coordinates of the *X*- and *Z*-axis immediately before the skip.

In order to ensure the accuracy and certainty of the LTO2S experimental data extraction, the contact measurement was implemented 50 times on the basis of the correction criteria using a standard circular gauge (50 mm, precision with 1 μm) to locate one-way recurrence and was examined with standard compasses. The results show that the average errors on both the *X*-axis and the *Z*-axis are within 1.5 μm, implying good structural rigidity of the probe and high repeatability of the computation of the MACRO code.

Additional analysis of cumulative errors is required of the cutter change of position because the probe is fixed on the tool carrier. The machine in the experiment is a Model GCL-2L (Goodway Machinery Co.) whose positioning precision in the *X*- and *Z*-axis after compensation can reach 1 μm. According to the data obtained by measuring the same fixed datum, the average error of cutter change on the *X*-axis is 2 μm and on the *Z*-axis is 3 μm.

3.3 Data Extraction

The hardware architecture of the data extraction system employs an A/D 812 (Yuan-Hwa Electronic Co.) card, working with an interface code written using Boland C++, to convert the analogue signals of temperatures measured by an IC-AD590 sensor into digital signals before saving them in the file. The experiment shows that the highest temperature of the spindle bearing of the machine tool is about 50°C. Any higher temperature will destroy the bearing. Let 50°C equal an IC-AD590 output voltage of 5 V, so the maximum input voltage is set to be ± 5 V, with a linearity of 25 mV (10V/4096). For the temperature sensor, in order to balance and reduce the voltage decrease caused by long-distance transmission and interference by external voltage signals, all the signal lines are isolated lines of the same length.

3.4 Experiment Framework

On the FANUC-OT controller used by the GCL-2L CNC turning centre it is easy to set the working coordinates. The overall method of the research is that a revolving speed meter tests the revolving speed of the spindle. The temperature measurement unit extracts the analogue signals of the temperatures by the IC-AD590 and converts them through the A/D card before the signals are saved in a personal computer file. The displacements measured by the displacement measurement unit are sent directly to the personal computer by means of an RS232 interface and saved in the file. Linear and nonlinear regression analyses are eventually carried out using SPSS [15] on all the information about temperature and displacement to obtain the relationship equation.

4. Analysis of Thermal Drift Behaviour for the Turning Centre

The thermal deformation analysis models for the turning centre can be divided into static analysis models and dynamic analysis models. The static analysis creates high temperature only through movement of the *X*- and *Z*-axes and the spindle revolution, and then further studies the relationship between temperature rise and thermal displacement. The study of the relationship between temperature rise and error based on real turning is called dynamic analysis. Generally, only the static model has been studied because it is easy to create a high temperature to measure and analyse, considering only a few variable coefficients. On the other hand, the dynamic model considers much more sophisticated variables. For example, the temperature distribution of the whole turning temperature site, the cutting tool's wear and tear in the turning process, machine vibration, heat from the friction between cutting tool and component part, and error undercutting real forces, and so on. This paper is an extension of [10], using S45C medium carbon steel as the test material, and actually measures the thermal deformation during real turning by experiment. It develops a set of systematic experimental methods, and proposes a series of modelling techniques for fast analysis of thermal errors and compensation methods applicable to a real processing environment which has the requirement for high precision.

4.1 Static Thermal Drifts of the Turning Centre

A standard testing rod is inserted into the chuck to measure the deformation of the testing rod by changing the spindle speed. To ensure circularity, the flatness of the end face, the repeatability of the LTO2S probe, and the errors caused by the environment of the standard testing rod, the radial and length deformation are measured by the average of three fixed points from the angles with 120° movements. The experiment was carried out at 500, 1000, 1500, 2000, 2500 and 3000 r.p.m. cutting speeds. The results show the distribution of temperatures and thermal errors for the static experiment is similar to the bearing's temperature increase relationships from the empirical equation in the bearing's technical manual. That is, the higher the revolving speed, the higher the temperature rise; however, beyond a certain high revolving speed, the temperature rise gradually approximates to a fixed level. Figure 1 shows the standard static relationship of temperature rise and thermal errors.

In the static analysis model, the location with the highest temperature rise is at the tail end of the spindle. Its temperature rises with the increase in the spindle speed, but eventually approximates to a stable level. The maximum temperature level is lower than 50°C. The temperature increase at other locations is not so obvious. From the experiment, in the static model, the displacement of the standard testing rod in the *X*- or *Z*-direction is very small, i.e. close to zero after deduction of the cutter change errors. The data from the static analysis show that it is not necessary to build a thermal error model for static or light machining. But does this mean that the lathe's thermal distribution or temperature rise will not affect the precision of machining? Real cutting will be carried out to test the relationship between thermal or temperature rise and errors in idle running and actual cutting.

4.2 Thermal Errors of Actual Cutting at the Turning Centre

In order to provide the same datum for machining and measuring, pre-experiment adjustment and correction must be done accurately, and appropriate control over material and the environment is also required. The following assumptions are made:

1. A large amount of cutting liquid is used in the machining process and the thermal deformation between cutting tool and component parts in the machining process is ignored.
2. The *X*- and *Z*-axial offset errors of the ball screws are already corrected by the controller parameters.

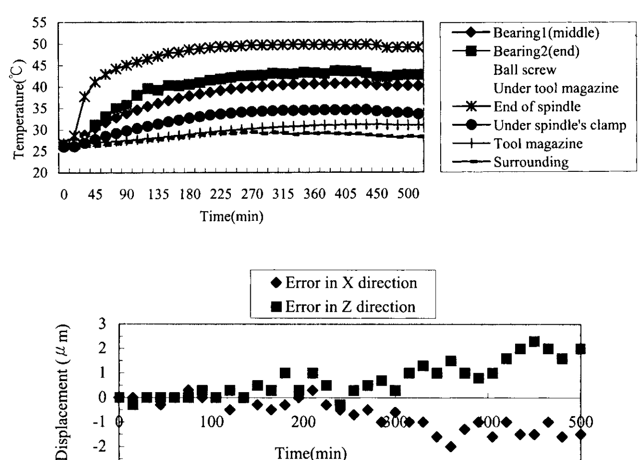

Fig. 1. The standard thermal drift with 3000 r.p.m. without real cutting.

3. A disposable cutting tool is used and the tool wear is ignored.
4. The cutting tool's positioning errors are already corrected.
5. The errors caused by cutter change are deduced by the average value in the experiment.
6. Environmental impact is ignored, for instance, magnetic field, change in humidity, and vibration.
7. The heat transmission is considered uniform and a consistent temperature is maintained for the machining site.

The experiment uses the G92 fixed turning C-code for the real cutting. The feed value *F* for turning refers to the suggested value of 0.25 mm rev^{-1} ~ 0.35 mm rev^{-1} for S45C medium carbon steel [16]. In order to study the impact that the feed value has on spindle temperature rise, this part of the experiment uses the spindle speeds of 500, 1000, 2000 and 3000 r.p.m. relative to the static experimental environment, and the depth of cut (DOC) is fixed. The experimental results show that when the depth of cut and the speed are fixed, and the feed speed varies (0.25 mm rev^{-1} ~ 0.4 mm rev^{-1}), the increase in the spindle temperature is almost the same. This means that within the normal feed speed range, the feed speed has a weak association with the spindle temperature rise. The error distribution after the temperature stabilises (about 90 min) is about 3 μm, without much variation.

If the revolution speed *S* is fixed, the feed value *F* seems not to have much impact on any change of temperature rise and thermal error. In order to prove this phenomenon, the depth of cutting is changed to DOC = 0.1 mm, revolution speed S = 500 r.p.m., and feed F = 0.25–0.4 mm rev^{-1}. The experiment results in the same amount of temperature rise of the spindle, and the thermal errors increase to 6 μm.

Now that the feed F = 0.4 mm rev^{-1} is fixed, the depth of cutting varies as DOC = 0.5 mm, 1.0 mm, 2.0 mm, and 5.0 mm, compared to the early experimental results, the depth of cut is found to be closely associated with temperature rise and thermal deformation. The deeper the cut, the larger the thermal error. This phenomenon holds true until DOC > 2 mm when it stabilises. The time for the temperature to reach the stable level is relatively shortened to 45 min. When the speed S = 3000 r.p.m., DOC = 5 mm, the temperature rise and thermal error reach the maximum, where the thermal error could be as large as 9 μm. The results are shown in Fig. 2.

The following conclusions are drawn based on experimental results:

1. Within the normal feedrate range, the feedrate is very weakly associated with the rise in spindle temperature.
2. Revolution speed *S* and the depth of cut have a close and positive relationship with the rate of temperature rise and the thermal error. The larger the values of revolution speed *S* and the depth of cut, the faster the rise in temperature and the larger the thermal error.
3. The temperature rise and thermal error have a corresponding relationship to each other, therefore increase of speed *S* and the depth of cut can be applied to fast modelling techniques.
4. A maximum thermal error of 9 μm exists when the revolution speed is 3000 r.p.m. and the depth of cut DOC = 5.0 mm.

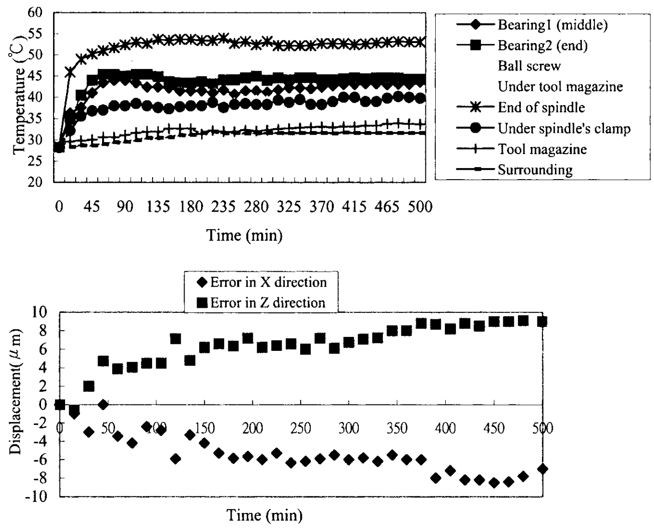

Fig. 2. The thermal drift at fixed $F = 0.4$ mm rev^{-1}, $S = 3000$ r.p.m., DOC $= 5$ mm without real cutting.

5. The relationship between temperature and thermal error under the conditions of idle running is quite different from that under the conditions of actual cutting. The model for temperature and thermal error can only be developed by means of actual cutting.
6. In the experiment, the thermal error is mainly caused by the spindle deformation when the spindle is heated.

4.3 Thermal Error Model for Spindle

By analysing the temperature rise at different points in actual cutting, it is found that the temperature change at all the points measured does not contribute to the overall thermal errors. Therefore, the key to cost-effective, simple, easy, and fast modelling is to locate the temperature points with the largest contribution and use these points as the source of the thermal errors caused by the rise in the spindle temperature.

4.3.1 Multivariable Regression Analysis

In regression analysis, the larger the correlation coefficient, the more consistent the relationship between the two. The least mean squares error represents the distance between the predicted values in the regression and the actual values. The smaller the error, the shorter the distance between the predicted values and the actual values. The correlation coefficient and the least mean square indicate the physical correlation or distance between the regression values and the actual values measured.

Regression analysis of X-axis. A regression analysis is run with the temperature and thermal error at individual and multivariable temperature levels, and the correlation between each temperature level and thermal error is observed. As shown by comprehensive analysis in Table 2, the thermal error is not caused by any single temperature level. The most highly correlated temperature level combination indicated by the correlation coefficients and least squares is T_1, T_2, and T_3, as shown in the equation below:

Table 2. Variable correlation comparison in regression for thermal errors on X-axis.

Regression variable	Correlation coefficient	Least squares error
T_1	0.7307	0.00641
T_2	0.8146	0.00702
T_3	0.7524	0.00789
T_4	0.5313	0.00672
T_5	0.5514	0.00684
T_6	0.5738	0.00690
T_7	0.5089	0.00868
T_8	0.7352	0.00636
T_1–T_8	0.8536	0.00588
$T_1T_2T_3T_8$	0.8769	0.00502
$T_1T_2T_3T_4$	0.8013	0.00563
$T_1T_2T_3T_4T_5$	0.7631	0.00571
$T_1T_2T_3T_4T_5T_6$	0.7951	0.00535
$T_1T_2T_3T_5$	0.8288	0.00521
$T_1T_2T_3T_5T_6$	0.8328	0.00508
$T_1T_2T_3T_7$	0.8041	0.00510
$T_1T_2T_4T_7T_8$	0.8143	0.00528
$T_2T_3T_4T_8$	0.7964	0.00569
$T_2T_3T_7T_8$	0.7990	0.00560
$T_3T_4T_5T_6$	0.7857	0.00539
$T_1T_2T_7T_8$	0.8011	0.00548
$T_1T_3T_5T_7T_8$	0.8122	0.00552

$$\Delta X_\epsilon = 8.6702 + 0.2167T_1 - 0.4419T_2 - 0.1508T_3 - 0.0676T_8 \quad (7)$$

Regression analysis of Z-axis. Z-axis regression analysis is done by directly using a combination and permutation of many temperature levels. In Table 3, the most highly correlated temperature combination indicated by the correlation coefficients and the least squares is T_1, T_2, and T_3, as shown in the equation below:

$$\Delta Z_\epsilon = -16.11748 + 0.44665T_2 - 0.23106T_3 + 0.28244T_8 \quad (8)$$

4.3.2 Nonlinear Regression Analysis

According to the experimental data, the working environment of light cutting (DOC $<$ 0.5 mm) has an impact on the spindle's temperature rise similar to static idle running, where the thermal errors exhibit a linear relationship. When DOC $\geq$ 0.5 mm, the trend of thermal errors can be represented by an exponential model. The simplified on-line compensation model can compute the displacement at a single temperature level. Hence, the relationship equation between temperature level and thermal error for rough machining is obtained from the nonlinear regression model.

X-axis regression analysis. To obtain the Pearson correlation coefficient and the least squares for the temperatures measured and the thermal errors, the strongest correlation is found at T_2, with the smallest least squares. The relationship equation between T_2 and the X-axis thermal error is thus established.

Table 3. Variable correlation comparison in regression for thermal errors on *Z*-axis.

Regression variable	Correlation coefficient	Least squares error
T_1	0.7907	0.00411
T_2	0.8198	0.00409
T_3	0.7411	0.00451
T_4	0.5967	0.00399
T_5	0.5122	0.00521
T_6	0.5813	0.00549
T_7	0.6011	0.00558
T_8	0.7744	0.00519
T_1–T_8	0.7892	0.00604
$T_1T_2T_3T_8$	0.7961	0.00598
$T_1T_2T_3T_4$	0.8694	0.00511
$T_1T_2T_3T_4T_5$	0.8011	0.00591
$T_1T_2T_3T_4T_5T_6$	0.7714	0.00583
$T_1T_2T_3T_5$	0.8107	0.00575
$T_1T_2T_3T_5T_6$	0.8233	0.00613
$T_1T_2T_3T_7$	0.8602	0.00513
$T_1T_2T_4T_7T_8$	0.7993	0.00600
$T_2T_3T_4T_8$	0.8459	0.00549
$T_2T_3T_7T_8$	0.8013	0.00581
$T_3T_4T_5T_6$	0.8121	0.00563
$T_1T_2T_7T_8$	0.7833	0.00588
$T_1T_3T_5T_7T_8$	0.7995	0.00566

When DOC $<$ 0.5 mm, the *X*-axis thermal error prediction model is depicted by the following equation, with the temperature at T_2 as the basis, and offset as the constant.

$$\Delta X_\epsilon = -0.31516\, T_2 + 9.56763 \tag{9}$$

When DOC $\geq$ 0.5 mm, the relationship between the temperature at T_2 and the thermal error obtained from the exponent model of the nonlinear regression analysis is illustrated as below:

$$\Delta X_\epsilon = -\, 7.33639 \exp\left(\frac{-2.11215}{T_2}\right) \tag{10}$$

Z-axis regression analysis. When DOC $<$ 0.5 mm, with the temperature at T_2 as the basis, the *Z*-axis thermal error prediction model is displayed as:

$$\Delta Z_\epsilon = 0.31045\, T_2 - 9.34764 \tag{11}$$

When the DOC $\geq$ 0.5 mm, the relationship between the temperature at T_2 and the thermal error obtained from the exponent model of the nonlinear regression analysis is as shown below:

$$\Delta Z_\epsilon = 8.95611 \exp\left(\frac{-5.08025}{T_2}\right) \tag{12}$$

5. Verification of the Thermal Error Model

The on-line compensation operating procedures are shown as Fig. 3. The OMP part of the LTO2S measurement system is mounted on the tool carrier. The measurements are based on recalling the cutting tool's NC codes. The LTO2S measurement

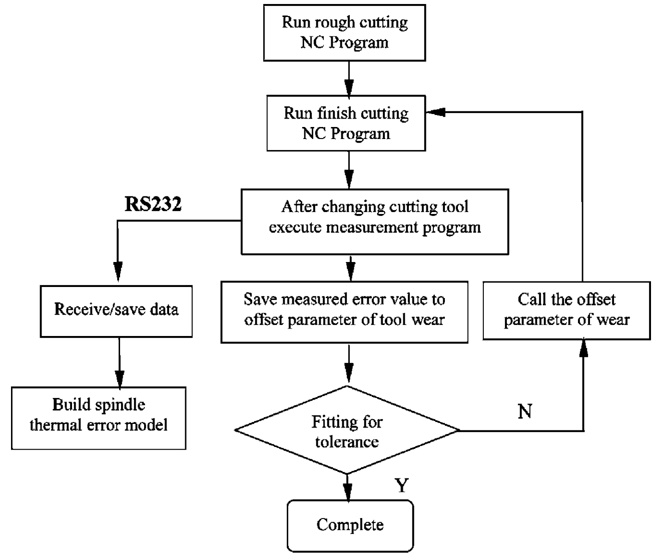

Fig. 3. The direct on-line compensation operating procedures.

system can be used for direct on-line compensation for spindle thermal deformation in processing. In executing LTO2S measurement codes, every action is written in the MACRO language, and then codes are called by G65 order to perform the measurement. The difference between the actual dimensions measured and the expected dimensions for processing can be saved in the correction parameters to offset the cutting tool wear, and sent to the personal computers through the RS232 transmission interface. When carrying out the next step in machining, by the means of a direct call for correction, that is, real-time on-line compensation for error, the machining error caused by heat and temperature rise of the spindle can be minimised. If there is no such equipment, then the relationship between the spindle's temperature rise and thermal error must be established before the machine is shipped out of the manufacturer's site. The focus of this paper is the software compensation for thermal errors. This refers to predicting the thermal error from the spindle temperature rise, transmitting the error values through an RS232 serial communication port to an external computer (or single chip) to correct the controller's parameters to offset the cutting tool wear, and call for correction parameters to realise prompt compensation.

Actual turning will be used to establish the different results before compensation and after actual on-line compensation. In order to compare the before and after results, the turning environment for testing refers to the thermal error experiment for actual cutting mentioned earlier. The error compensation procedure flowchart is shown in Fig. 4.

5.1 Empirical Test of the Multivariable Regression Model

Apply the thermal errors obtained from multivariable regression analysis, and the single part temperatures measured in the real cutting environment, to the Eqs (7) and (8), to obtain the *X*- and *Z*-axis error values. Then put these error values into the correction parameter for the cutting tool wear, and call this

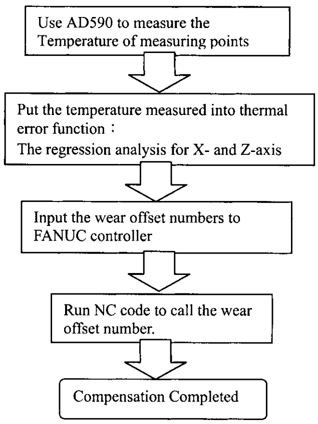

Fig. 4. The error compensation procedure flowchart.

parameter in turning to execute on-line compensation. As shown in Fig. 5, the real-time compensation based on the thermal errors obtained from multivariable regression analysis can reduce the average errors to below 60%. Notably, in the early stage of compensation, because the distance constant in the compensation equation in the multivariable regression model is a regression constant under different temperatures, the initial value of the temperature is the room temperature when the machine tool is turned on. This constant will cause over compensation, requiring the temperature differential to be compensated.

5.2 Empirical Test of the Nonlinear Regression Model

Combine the thermal errors obtained from the linear and nonlinear regression models, execute on-line compensation by the relationship Eqs (9)–(12). In the real cutting environment, when DOC $<$ 0.5 mm, the X- and Z-axis thermal error–temperature relationship equations are replaced by Eqs (9) and (11). When DOC $\geq$ 0.55 mm, the X- and Z-axis thermal error–temperature relationship equations are replaced by Eqs (10) and (12). The experimental results are shown in Figs 6 and 7. Real-time compensation by executing the thermal error compensation equations combining the single-variable linear and nonlinear regression models can reduce the average errors to below 40%. When DOC $<$ 0.5 mm, the test results when the cutting first starts are the same as those described in Section 5.1.

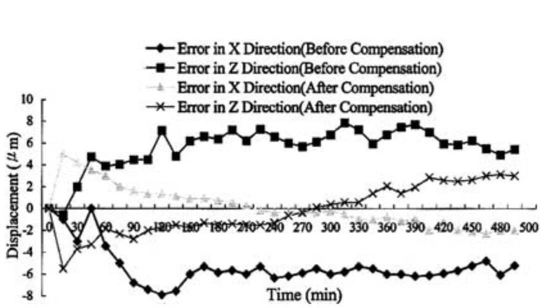

Fig. 5. Multivariable linear regression compensation with S = 3000 r.p.m., F = 0.4 mm rev^{-1}, DOC = 5.0 mm in real cutting.

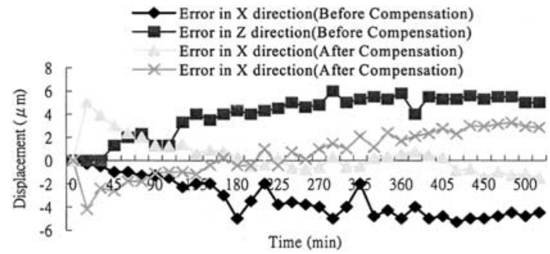

Fig. 6. Nonlinear regression compensation with S = 3000 r.p.m., F = 0.4 mm rev^{-1}, DOC = 0.1 mm when DOC $<$ 0.5 mm.

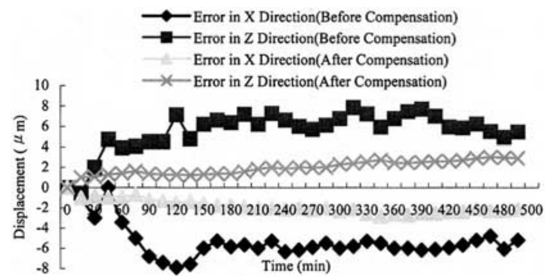

Fig. 7. Nonlinear regression compensation with S = 3000 r.p.m., F = 0.4 mm rev^{-1}, DOC = 0.1 mm when DOC $\geq$ 0.5 mm.

6. Conclusion

The machining errors caused by the rise in spindle temperature in finish machining cannot be taken for granted. This work proposes a series of fast measuring techniques and on-line real-time compensation methods for thermal deformation due to the spindle temperature rise. When comparing the thermal error compensation values obtained from multivariable linear regression and by combining the single-variable linear regression and nonlinear exponential models, the on-line compensation based on the former relationship Eq. can reduce the average errors to below 60% while the latter can reduce the errors to below 40%. The conclusion from the experimental results is when the spindle thermal error–temperature model for the turning centre is established, if linear and nonlinear regression models are combined, the trends of temperature rise and thermal error in the cases of light cutting and heavy cutting are differentiated, the optimal model for spindle thermal errors can be obtained. Application of this model for actual on-line compensation can help achieve the ultimate goals of accurate modelling, fast real-time compensation, finish machining, and improved product quality. Eventually, if the thermal error compensation model can be recorded on a single chip (i.e. 8051 or DSP), the PC can be replaced by a single chip computer for error compensation, and then the costs of thermal error compensation techniques can be reduced.

Acknowledgement

This research is under National Science Consult contract of NSC87-2218-E-005-006.

References

1. J. B. Bryan, “International status of thermal error research”, Annals CIRP, 16, 1968.
2. J. B. Bryan, “International status of thermal error research”, Annals CIRP, 39(2), 1990.
3. J. S. Chen, “Real-time compensation for time-variant volumetric error on a machine center”, Transactions ASME, 115, November 1993.
4. K. Okushima, “Compensation of thermal displacement by coordinate system correction”, Annals CIRP, 24(1), pp. 327–331, 1975.
5. R. Schultschik, “Possibilities and limits of error feedback in automatic machining”, Annals CIRP, 30(1), pp. 467–471, 1981.
6. M. Barash, “Thermal effects on the accuracy of numerically controlled machine tools”, Annals CIRP, 35(1), pp. 255–258, 1986.
7. P. C. Tseng, “Thermal compensation on a machining center”, International Journal of Advanced Manufacturing Technology, 13, pp. 182–190, 1997.
8. Y. Takeuchi et al. “Improvement in the working accuracy of an NC lathe by compensation for thermal expansion”, Precision Engineering, 14(1), pp. 19–24, 1982.•<aq1>•
9. M. Shirashi, “Geometrical adaptive control in NC turning operation”, Journal of Engineering for Industry, 106, February 1984.
10. L. C. Lin, “The study of thermal error on turning center”, 13th Proceeding of Chinese Mechanical Engineering, pp. 314–321, 1996.
11. A. M. Domez, “A general methodology for machine tool accuracy enhancement: theory, application, and implementation”, PhD dissertation, Purdue University, 1985.
12. O. Kilicay, “The thermal distortion of machine tools: general information and data research”, report No. 87, Confidential to Members of Mtira, pp. 4–60, 1982.
13. T. V. Vorburger and B. R. Scace, “Progress report of the quality in automation project for FY89”, pp. 9–48, 1990.
14. A. H. Slocum, Precision Machine Design, 2nd edn, pp. 274–278, Prentice-Hall, 1992.
15. E. Mansfield, Statistics for Business and Economics: Methods and Applications, 5th edn, pp. 450–547, W. W. Norton, 1994.
16. ASTM, Metals Handbook Volume 1, ASTM International, pp. 8–647, 1990.